Therapeutic effects of paeonol on non-small cell lung cancer cells via regulation of the MAPK pathway

WEN GAN, CHONG CHEN, MIAOLONG HUANG and YOUTAO LI

Department of Thoracic Surgery, Yuebei People Hospital Affiliated to Medical College of Shantou University, Shaoguan, Guangdong 512000, P.R. China

Received May 13, 2024; Accepted August 16, 2024

DOI: 10.3892/ol.2024.14693

Abstract. The present study aimed to investigate the molecular mechanisms by which paeonol impedes DNA damage repair, induces apoptosis and inhibits cell viability via the mitogen-activated protein kinase (MAPK) pathway. Firstly, normal human bronchial epithelial cells (BEAS-2B) and non-small cell lung cancer cells (H1299) were employed in the study as cellular models. Following cultivation, the cells were divided into experimental and control groups, and were treated with different concentrations of paeonol. Subsequently, various techniques, including western blotting, Cell Counting Kit-8, colony formation, TUNEL and comet assays were conducted to evaluate the effects of paeonol on cell viability, colony-forming ability, apoptosis levels and DNA damage in H1299 cells. According to the experimental results, paeonol significantly reduced the viability and colony formation ability of H1299 cells, but substantially increased apoptosis and DNA damage. These effects were enhanced in response to higher concentrations of paeonol. Furthermore, western blot analysis revealed that paeonol treatment decreased the protein levels of B-cell lymphoma 2 and breast cancer susceptibility gene 1, while it increased the expression levels of cleaved-PARP, cleaved-caspase 3, γH2AX and P21. Additionally, the phosphorylated levels of extracellular signal-regulated kinase 1, c-Jun N-terminal kinase and P38 within the MAPK signaling pathway were diminished. Collectively, the present study demonstrated that paeonol may inhibit the metabolic activity and proliferative capability of H1299 cells, and that it could promote apoptosis and obstruct DNA damage repair by modulating the MAPK signaling pathway.

Correspondence to: Professor Youtao Li, Department of Thoracic Surgery, Yuebei People Hospital Affiliated to Medical College of Shantou University, 133 Huimin South Road, Shaoguan, Guangdong 512000, P.R. China
E-mail: 18023698576@163.com

Key words: paeonol, mitogen-activated protein kinase pathway, apoptosis, DNA damage repair, non-small cell lung cancer

Introduction

Due to an aging population and changes in lifestyle, the global burden of cancer is escalating, placing significant pressure on health systems worldwide (1). Non-small cell lung cancer (NSCLC), one of the most prevalent types of lung cancer, is characterized by high incidence and mortality rates (2). Compared with small cell lung cancer, NSCLC exhibits fundamental differences in treatment and prognosis; therefore, exploring novel compounds capable of effectively inhibiting tumor proliferation and inducing apoptosis is of great importance for enhancing cancer treatment efficacy and improving survival rates (3).

Paeonol, a phenolic compound discovered in plants such as peonies, exhibits a broad range of biological activities, including analgesic, anti-inflammatory, antipyretic and anti-allergic effects (4). In rat models of Alzheimer's disease, paeonol increases antioxidant enzyme levels and reduces pro-inflammatory factors in the hippocampus, helping to alleviate cognitive impairments in Alzheimer's disease (5). The potential of paeonol in the treatment of various tumors, particularly through modulation of the mitogen-activated protein kinase (MAPK) pathway, has become a focal point in cancer treatment research. The MAPK pathway, which is essential for cellular functions such as proliferation, differentiation, migration, survival and apoptosis, involves a cascade of protein kinases that sequentially activate downstream molecules and ultimately affect gene expression. Based on the core constituent protein kinases, the MAPK pathway consists of several major branches, including extracellular signal-regulated kinase 1 (ERK1), c-Jun N-terminal kinase (JNK) and P38 MAPK pathways, which each serve a role in various physiological and pathological processes. Under normal physiological conditions, the MAPK pathway assists cells in adapting to external stimuli, maintaining cellular function and tissue homeostasis. However, in pathological conditions such as cancer, abnormal activation or inhibition of this pathway can lead to uncontrolled cell proliferation, suppression of apoptosis, and enhanced tumor invasion and metastasis (6). Therefore, understanding the regulatory mechanisms of the MAPK pathway is essential for developing new therapeutic strategies.

In recent years, growing research has focused on the inhibitory effects of natural products on tumor cells, with

paeonol attracting attention for its demonstrated antitumor activity in various cancer models. By intervening with the MAPK pathway, paeonol may affect cell cycle regulation, DNA damage repair processes and activation of apoptotic signaling, thereby exhibiting a dual inhibitory effect on tumor cells. Particularly by hindering DNA damage repair mechanisms, paeonol may enhance the sensitivity of tumor cells to chemotherapeutic drugs, offering a new strategy for cancer treatment (7,8). Numerous studies have also shown that paeonol exhibits broad-spectrum anticancer effects through multiple molecular pathways, including PI3K/AKT (9), NF-κB (10), Wnt/β-catenin (11), MAPK (12) and TGF-β/Smad (13), and several microRNAs, such as miR-126-5p, miR-139-5p and miR-665 (14-16). These pathways contribute to inhibiting cell proliferation, invasion and migration, inducing apoptosis and cell cycle arrest, and modulating immune suppression and inflammatory responses within the tumor microenvironment, further highlighting the anticancer potential of paeonol.

The present study aimed to explore the molecular mechanisms by which paeonol may inhibit DNA damage repair, induce apoptosis and suppress proliferation through the MAPK pathway. In addition, the present study evaluated the differential impacts of paeonol at various doses on H1299 cells. The findings of the present study may provide a scientific foundation for the application of paeonol in cancer therapy.

Materials and methods

Cell culture and treatment. BEAS-2B normal human bronchial epithelial cells were supplied by Beyotime Institute of Biotechnology, and H1299 NSCLC cells were provided by Wuhan Pricella Biotechnology Co., Ltd. BEAS-2B cells were cultured in Bronchial Epithelial Growth Medium (Lonza Group, Ltd.) supplemented with 2.0 mg/l bovine pituitary extract (Gibco; Thermo Fisher Scientific, Inc.), 0.5 mg/l hydrocortisone, 0.5 mg/l human epidermal growth factor (Sigma-Aldrich; Merck KGaA), 0.5 mg/l epinephrine and 0.5 mg/l transferrin. H1299 cells were cultured in Roswell Park Memorial Institute 1640 Medium (Thermo Fisher Scientific, Inc.) supplemented with 10% fetal bovine serum (Sigma-Aldrich; Merck KGaA), 1% penicillin-streptomycin, 10.0 mg/l glycine, 1.0 mg/l folic acid and 100.0 mg/l calcium nitrate. The cell culture conditions were maintained at 37˚C and 5% CO_2.

Paeonol (MedChemExpress) was dissolved in a solution consisting of dimethyl sulfoxide and 20% sulfobutylether-β-cyclodextrin (MedChemExpress) in saline (10/90, v/v). To assess the cytotoxic effects of paeonol, BEAS-2B and H1299 cells were allocated into six groups and exposed to increasing concentrations of paeonol (0, 20, 40, 60, 80 and 100 μg/ml) for at 37˚C for 24 h. For further analysis, H1299 cells were specifically grouped and treated with different concentrations of paeonol at 37˚C for 24 h; the groups were as follows: i) Control group: H1299 cells treated with 0 μg/ml paeonol; ii) 20 μg/ml group: H1299 cells treated with 20 μg/ml paeonol; iii) 40 μg/ml group: H1299 cells treated with 40 μg/ml paeonol; iv) 80 μg/ml group: H1299 cells treated with 80 μg/ml paeonol.

Cell Counting Kit (CCK)-8 assay. The CCK-8 assay kit (Beyotime Institute of Biotechnology) was employed to assess cell viability and cytotoxicity. Briefly, BEAS-2B and H1299 cells were seeded at an appropriate density of $5x10^3$ cells/well in 96-well plates. Subsequently, 10 μl CCK-8 solution was added to each well and the plates were incubated in a cell culture incubator at 37˚C and 5% CO_2 for 2 h until a noticeable color change occurred in the wells. The optical density was then determined at a wavelength of 450 nm using a microplate reader (Thermo Fisher Scientific, Inc.) to evaluate cell viability or cytotoxicity (17).

Cell colony formation assay. After culturing H1299 cells to 80-90% confluence, they were detached and converted into a single-cell suspension through trypsin digestion. Subsequently, the cells were diluted to an appropriate density of 500 cells/well and cultured at 37˚C and 5% CO_2 until visible colonies formed. Upon removal of the culture medium, the cells were fixed with 100% methanol at room temperature for 20 min and stained with 1 ml Giemsa stain (Beyotime Biotechnology, China) at room temperature for 30 min. Finally, visible colonies were counted under a light microscope, where colonies were defined as clusters containing >50 cells. Both the number and size of the colonies were recorded to assess the colony formation ability of H1299 cells.

TUNEL assay. The TUNEL assay kit (Beyotime Institute of Biotechnology) was utilized to evaluate apoptosis. Specifically, H1299 cells were fixed with 4% formaldehyde solution at room temperature for 15-30 min, followed by washing with PBS. After treatment with proteinase K, the samples were incubated with a mixture of biotinylated deoxyuridine triphosphate and terminal deoxynucleotidyl transferase under suitable reaction conditions at 37˚C for 1 h. After incubation, 4',6-diamidino-2-phenylindole was added at a concentration of 1 μg/ml for staining, and the samples were incubated at room temperature for 5-10 min. Next, the samples were analyzed using a fluorescence microscope (Thermo Fisher Scientific, Inc.) to assess the level of apoptosis. A minimum of five fields of view were observed to determine the number of TUNEL-positive cells, which indicate significant DNA fragmentation, evident through enhanced fluorescence or color development (18).

Comet assay. The comet assay kit (Beyotime Institute of Biotechnology) was employed to assess the DNA damage in H1299 cells. Briefly, the cells were collected at a density of $1x10^5$ cells/ml and embedded in low melting point agarose. The cells embedded in agarose were then pipetted onto a microscope slide precoated with a layer of agarose, and were overlaid with a third layer of agarose to encapsulate the cells. Upon solidification, the slides were immersed in lysis solution at 4˚C to lyse the cells, thereby removing the cell membrane and part of the nuclear proteins to release the DNA. After lysis, the slides were transferred to an electrophoresis tank and subjected to electrophoresis, under alkaline conditions. During this process, fragmented DNA and relaxed DNA migrated towards the anode, forming a 'comet tail'. After electrophoresis, the slides were washed with water or alcohol and then stained with 20 μg/ml ethidium bromide at room temperature for 15 min for visualization. Under a fluorescence microscope, the DNA in the comet's head (unaltered DNA) and tail (damaged DNA) was

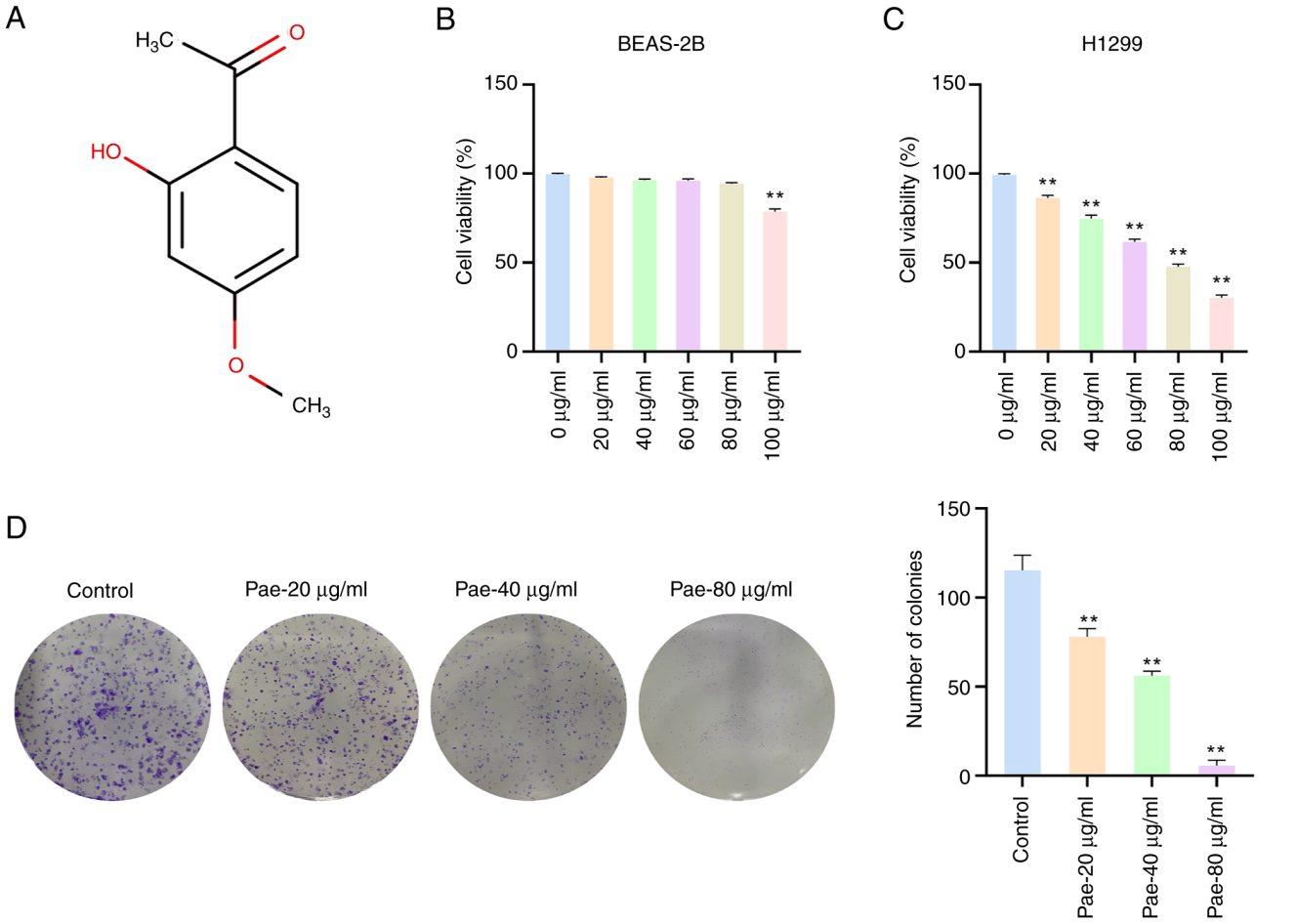

Figure 1. Effects of Pae on cell viability and proliferation. (A) Chemical structure of Pae. Determination of the effect of Pae on the viability of (B) BEAS-2B and (C) H1299 cells, as determined by Cell Counting Kit-8 assay. (D) Effects of Pae on the proliferative ability of H1299 cells, as determined by cell colony formation assay. n=3. **P<0.01 vs. control group. Pae, paeonol.

observed, analyzed and images were captured. The percentage of tail DNA (%) and tail moment were calculated using specialized software (Comet Assay Software Version 1.2.3; Trevigen, Inc.; Bio-Techne), where tail DNA (%) was determined by the ratio of the fluorescence intensity in the tail to the total fluorescence intensity, and tail moment was calculated as the product of the tail length and the percentage of DNA in the tail.

Western blotting. The cells were lysed with RIPA lysis buffer (Beyotime Institute of Biotechnology) and proteins were quantified using the Bradford protein assay kit (Beyotime Institute of Biotechnology). The proteins (40 μg/lane) were then separated by sodium dodecyl sulfate-polyacrylamide gel electrophoresis on a 10 or 12% gel, followed by transfer onto polyvinylidene fluoride membranes. After blocking with 5% non-fat milk at room temperature for 2 h, the membranes were incubated with specific primary antibodies overnight at 4˚C: B-cell lymphoma 2 (Bcl-2; 1:1,000; cat. no. ab194583), cleaved-PARP (1:1,000; cat. no. ab4830), PARP (1:1,000; cat. no. ab32064), caspase 3 (1:5,000; cat. no. ab32351), cleaved-caspase 3 (1:5,000; cat. no. ab214430), γH2AX (1:1,000; cat. no. ab243906), H2AX (1:1,000; cat. no. ab229914), breast cancer susceptibility gene 1 (BRCA1; 1:1,000; cat. no. ab90528), P21 (1:1,000; cat. no. ab109199), JNK (1:2,000; cat. no. ab124956), phosphorylated (p)-JNK (1:2,000; cat. no. ab124956), P38 (1:1,000; cat. no. ab316937), p-P38 (1:1,000; cat. no. ab4822), ERK1 (1:1,000; cat. no. ab32537), p-ERK (1:1,000; cat. no. ab201015) and GAPDH (1:10,000; cat. no. ab181603) (all from Abcam). The membranes were then incubated with horseradish peroxidase-labeled secondary antibodies (1:5,000; cat. no. ab205718; Abcam) at room temperature for 1 h. By adding an enhanced chemiluminescence substrate (cat. no. 32109; Thermo Fisher Scientific, Inc.), a chemiluminescent reaction was triggered, producing luminescent signals that were detected via fluorescence imaging system. Semi-quantitative analysis of the protein bands was conducted based on their intensity using ImageJ 5.0 software (National Institutes of Health) (19).

Statistical analysis. Statistical analysis was performed using SPSS 26.0 software (IBM Corporation). The data are presented as the mean ± standard deviation and each experiment was repeated at least three times. Group differences were evaluated using one-way ANOVA followed by Tukey's post hoc test for multiple comparisons. P<0.05 was considered to indicate a statistically significant difference.

Results

Effects of paeonol on cell viability and proliferation. The effects of paeonol (Fig. 1A) on viability and proliferation were

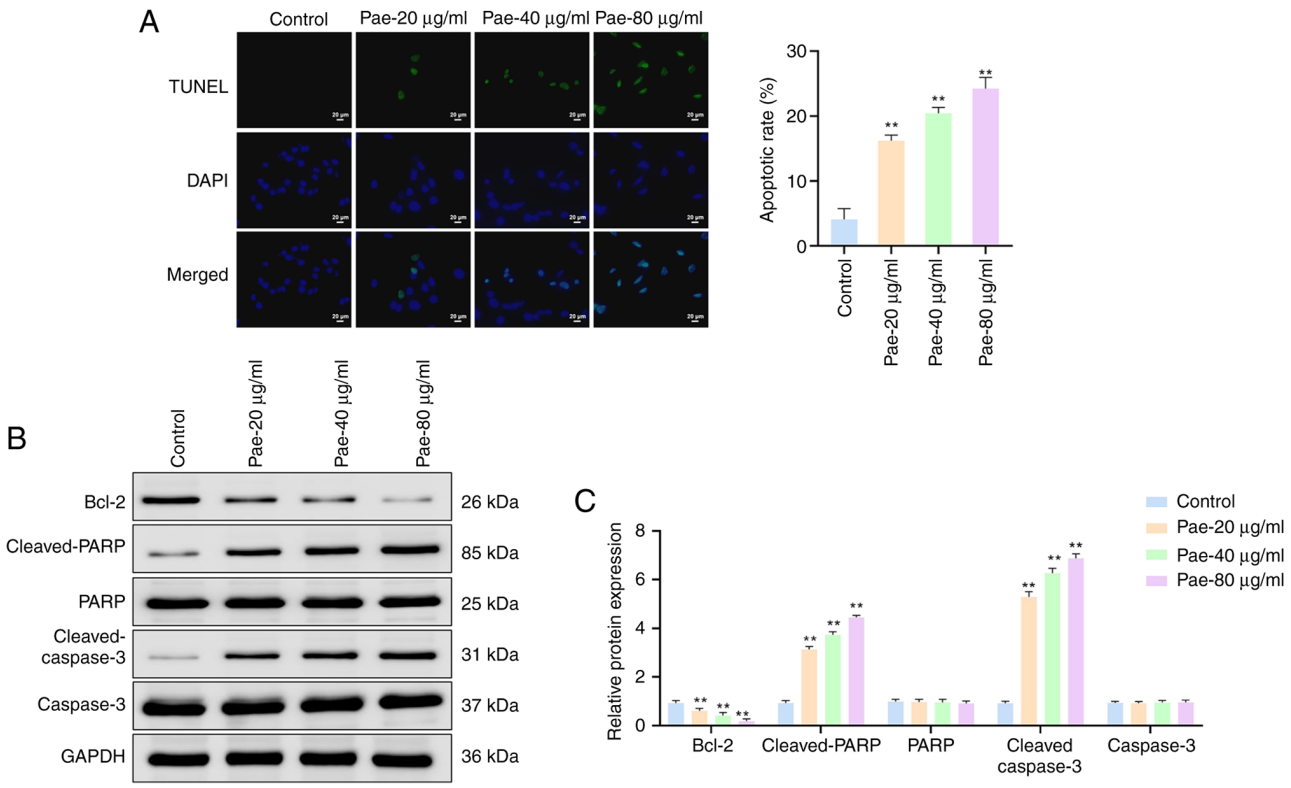

Figure 2. Pae promotes the apoptosis of H1299 cells. (A) Apoptosis of H1299 cells was determined by TUNEL assay. (B) Protein expression levels of Bcl-2, cleaved-PARP, PARP, cleaved-caspase 3 and caspase 3 in H1299 cells were determined by western blot analysis. (C) Semi-quantification of relative protein expression levels for Bcl-2, cleaved-PARP, PARP, cleaved-caspase 3 and caspase 3 in H1299 cells. n=3. **P<0.01 vs. control group. Bcl-2, B-cell lymphoma 2; Pae, paeonol.

evaluated through CCK-8 and cell colony formation assays. The results of CCK-8 assay (Fig. 1B) indicated that paeonol did not exhibit significant cytotoxicity to BEAS-2B cells within the concentration range of 0-80 μg/ml, as cell viability remained comparable to the control. However, paeonol treatment significantly decreased the viability of H1299 cells in a dose-dependent manner (P<0.01; Fig. 1C), suggesting a toxic effect on these cells. Additionally, the cell colony formation assay (Fig. 1D) further confirmed the inhibitory effect of paeonol on the proliferative capability of H1299 cells. While the CCK-8 assay primarily reflected overall cell viability and survival, the colony formation assay directly measured the proliferative capacity of cells. The results showed a significant dose-dependent reduction in colony formation ability of H1299 cells treated with paeonol (P<0.01), indicating that paeonol effectively reduced the proliferative capacity of these cells. These findings suggested that paeonol exerted a toxic effect on H1299 cells, primarily by inhibiting their proliferative capacity.

Paeonol promotes the apoptosis of H1299 cells. Subsequently, TUNEL assays and western blot analysis were performed to investigate the pro-apoptotic effects of paeonol on H1299 cells. The TUNEL assay results revealed a concentration-dependent increase in apoptosis levels among H1299 cells treated with paeonol compared with the control group (P<0.01; Fig. 2A). Western blot analysis further supported these findings, demonstrating significant dose-dependent increases in the expression levels of apoptosis-inducing proteins (cleaved-PARP and cleaved-caspase 3) (P<0.01), with no significant changes in the expression of PARP and caspase 3 (Fig. 2A and B). Additionally, there was a significant decrease in the expression levels of the anti-apoptotic protein Bcl-2 (P<0.01). These changes in protein expression suggested that paeonol effectively regulated apoptotic signals.

Paeonol inhibits DNA damage repair in H1299 cells. The comet assay was used to assess the impact of paeonol on DNA damage in H1299 cells. According to the assay results, there was a significant increase in DNA damage across all concentrations of paeonol, as evidenced by enhanced comet tail DNA content and length (P<0.01; Fig. 3A-C). Furthermore, western blot analysis was employed to measure the expression levels of proteins associated with DNA damage and cell cycle regulation. The analysis results showed a significant increase in the expression levels of the DNA damage marker γH2AX/H2AX and cell cycle inhibitor P21 in H1299 cells, alongside a significant decrease in the expression levels of the DNA repair protein BRCA1 (P<0.01; Fig. 3D and E). These changes suggested that paeonol induced cell cycle arrest and diminished DNA damage repair capacity in H1299 cells.

Paeonol inhibits the MAPK pathway in H1299 cells. Western blot analysis was applied to evaluate the effect of paeonol on the MAPK signaling pathway in H1299 cells. The analysis focused on the levels of p-ERK1/ERK1, p-JNK/JNK and p-P38/P38, comparing cells treated with various concentrations of paeonol to the control group. The analysis results indicated that paeonol treatment led to a significant decrease

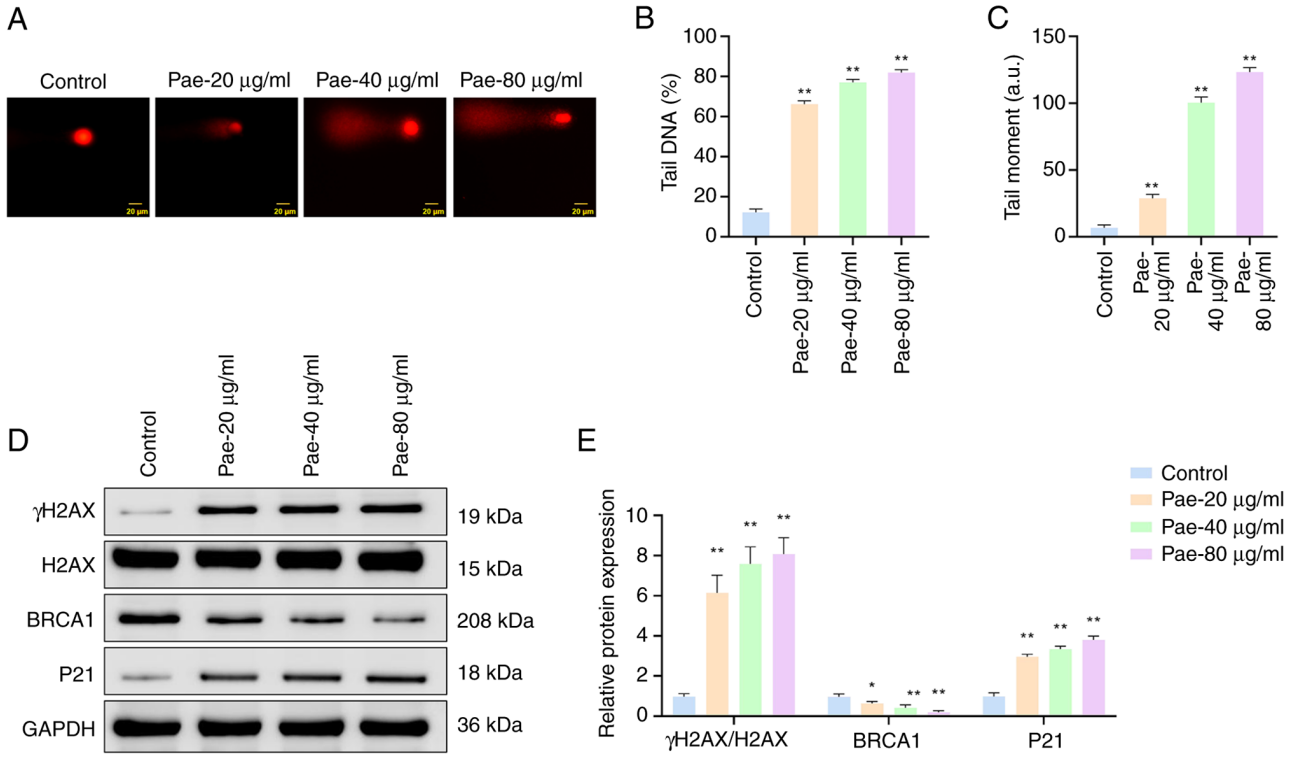

Figure 3. Pae inhibits DNA damage repair in H1299 cells. (A) Determination of the impact of Pae on DNA damage in H1299 cells, as determined by comet assay (magnification, x400). (B) Comet tail DNA content in H1299 cells. (C) Comparison of tail moment in H1299 cells. (D and E) Protein expression levels of γH2AX/H2AX, BRCA1 and P21 in H1299 cells were detected by western blotting. n=3. *P<0.05, **P<0.01 vs. control group. BRCA1, breast cancer susceptibility gene 1; Pae, paeonol.

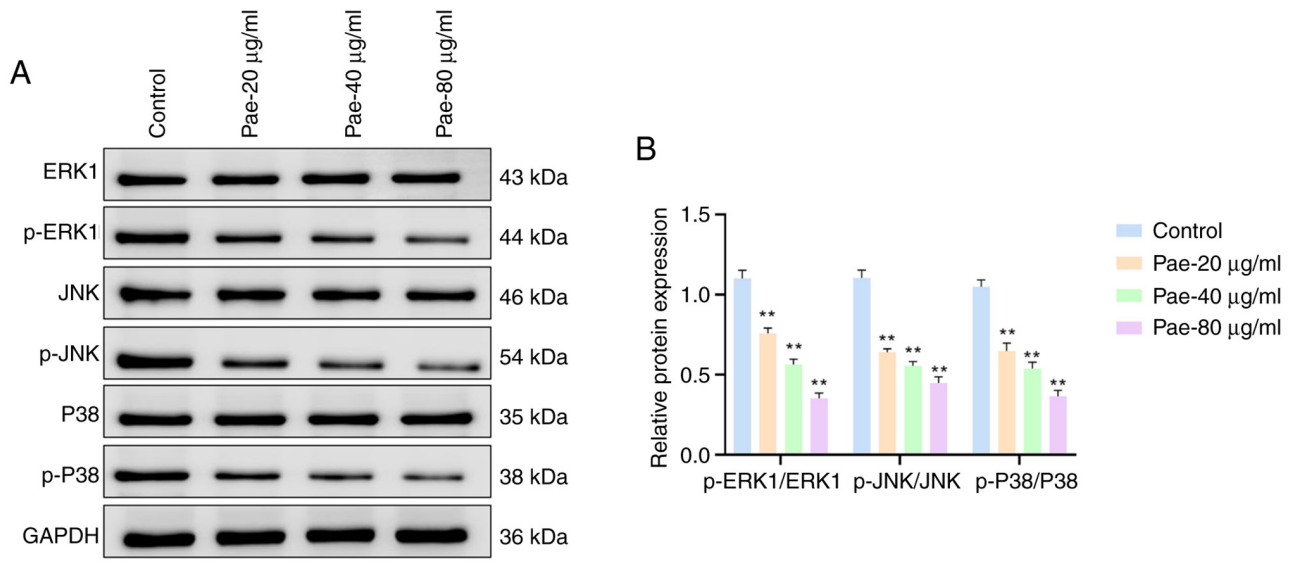

Figure 4. Pae inhibits the mitogen-activated protein kinase pathway in H1299 cells. (A) Protein expression levels of ERK1, p-ERK1, JNK, p-JNK, P38 and p-P38 in H1299 cells were detected by western blot analysis. (B) Relative protein expression levels of p-ERK1/ERK1, p-JNK/JNK and p-P38/P38 in H1299 cells. n=3. **P<0.01 vs. control group. ERK, extracellular signal-regulated kinase; JNK, c-Jun N-terminal kinase; Pae, paeonol.

in the phosphorylation of ERK1, JNK and P38 at all tested concentrations compared with the control group (P<0.01), with no notable changes in the expression of total proteins (ERK1, JNK and P38) (Fig. 4A and B). We assessed one of the splice variants of JNK, along with its phosphorylation state, which corresponded to molecular weights of 46 and 54 kDa, respectively. These outcomes suggested that paeonol effectively inhibited activation of the MAPK pathway, potentially leading to the apoptosis and reduced proliferation of H1299 cells.

Discussion

Previous studies have demonstrated that paeonol has various anticancer mechanisms in NSCLC and lung adenocarcinoma,

including upregulation of tumor suppressor genes, regulation of glycolytic reprogramming, disruption of key signaling pathways and enhancement of radiosensitivity (20-22). Notably, paeonol has been shown to inhibit the *in vitro* migration and invasion of A549 lung cancer cells, and to reduce the secretion of inflammatory cytokines (23-25). In NSCLC cells, paeonol has been reported to exhibit significant anticancer activity by upregulating the expression of the tumor suppressor genes TNNC1 or SCARA5, leading to inactivation of the AKT signaling pathway (23-25). Additionally, paeonol may regulate glycolytic reprogramming and proliferation in A549 cells through m6A modification of ACADM (23-25). Paeonol can also effectively inhibit the proliferation, migration and invasion of NSCLC cells by disrupting the STAT3 and NF-κB signaling pathways, suggesting its potential as a promising anti-metastatic agent for cancer chemotherapy (21). Moreover, paeonol has been reported to enhance radiation-induced apoptosis and inhibit the PI3K/Akt pathway, demonstrating radiosensitizing effects in lung adenocarcinoma (26).

Building on these aforementioned findings, the present study investigated the effects of paeonol on the viability, apoptosis and DNA damage of H1299 cells. Due to the lack of existing data on paeonol in H1299 cells, the doses were selected based on preliminary experimental results and dose-response curves. Our preliminary experiments assessed the effects of different concentrations of paeonol on cell viability, proliferation and apoptosis, helping to determine the dose range (20, 40 and 80 μg/ml) used in the present study. The present findings demonstrated that paeonol inhibited the viability and induced the apoptosis of H1299 cells. Additionally, paeonol effectively disrupted DNA repair, which may increase cell sensitivity to DNA damage. In addition, paeonol suppressed the MAPK pathway, potentially contributing to its anti-proliferative and pro-apoptotic effects, with these effects showing a clear concentration dependency.

Previous research has shown that paeonol can directly target tumor cells, inhibiting cell division and proliferation during the G_0/G_1 or G_2/M phases, and triggering apoptosis through both intrinsic and extrinsic pathways (23-25). Consistent with previous findings, the present study further validated the potential value of paeonol in modulating apoptosis-related proteins and suppressing anti-apoptotic factors, such as Bcl-2 (20,21,27). Additionally, the MAPK pathway, comprising ERK1, JNK and P38 MAPK, has been reported to serve a pivotal role in various biological functions, including cell growth, cell cycle regulation, stress responses and apoptosis (28-30). The current study confirmed that paeonol was effective in inhibiting activation of the MAPK signaling pathway, which is considered one of the crucial cellular signal transduction pathways.

The present results not only corroborated the established antitumor activity of paeonol but also improved the understanding of its underlying mechanisms (31). For example, alterations in protein expression, such as downregulation of Bcl-2, and upregulation of cleaved-PARP and cleaved-caspase 3, indicated the apoptosis pathways influenced by paeonol. In terms of DNA damage repair, paeonol was observed to enhance the expression of the DNA damage marker γH2AX/H2AX and reduce the levels of the DNA repair protein BRCA1, which suggested a weakened DNA damage repair capability (22,32). Such effects could position paeonol as a promising chemosensitizer (14,33). The present study not only confirmed the antitumor activity of paeonol and revealed its potential molecular mechanisms, but also offered novel insights into regulation of the MAPK signaling pathway and its implications for other cancer types reliant on this pathway (16,34-36).

Despite the present study highlighting the antitumor potential of paeonol in H1299 cells, it is important to note that BEAS-2B is a normal human bronchial epithelial cell line, whereas H1299 is a NSCLC cell line. The differences in sensitivity to paeonol between BEAS-2B and H1299 cells may be attributed to inherent genetic and metabolic differences between normal and cancer cells. Additionally, cancer cells such as H1299 often exhibit dysregulated signaling pathways, including those involved in cell proliferation and apoptosis, which may make them more susceptible to the effects of paeonol.

The current study primarily utilized *in vitro* cell models (BEAS-2B and H1299 cells) to demonstrate the effects of paeonol. However, to further validate these findings, it is necessary to assess the variability in responses to paeonol among different types of NSCLC cells, and to conduct *in vivo* studies and clinical trials. Since this study used only one NSCLC cell line (H1299), it limits the comprehensive understanding of the efficacy of paeonol across various cancer subtypes. Although the impact of paeonol on the MAPK signaling pathway was identified, other signaling pathways or molecular mechanisms may also contribute to its antitumor effects, which require further investigation. Given these limitations, future research should aim to validate the antitumor effects of paeonol using *in vivo* models, and explore its safety profile and pharmacokinetics. In addition, attention should be given to testing the long-term effects and potential toxicity of paeonol. This will help to comprehensively understand the potential and application prospects of paeonol in cancer therapy.

In conclusion, the present study indicated that paeonol can effectively inhibit the metabolic activity and proliferative capacity of H1299 cells, promote apoptosis and impede DNA damage repair processes, which could be achieved through modulation of the MAPK signaling pathway. Furthermore, the present study improves the understanding of the mechanisms underlying the antitumor effects of paeonol, and lays a scientific foundation for further investigation of its anticancer activity *in vivo* and its potential application in clinical cancer treatment.

Acknowledgements

Not applicable.

Funding

No funding was received.

Availability of data and materials

The data generated in the present study may be requested from the corresponding author.

Authors' contributions

WG and YL conceived and designed the study, and conducted the study. CC and MH were involved in data acquisition, analysis and interpretation. WG and YL edited the manuscript draft, and reviewed and edited the manuscript. CC and MH confirm the authenticity of all the raw data. All authors read and approved the final version of the manuscript.

Ethics approval and consent to participate

Not applicable.

Patient consent for publication

Not applicable.

Competing interests

The authors declare that they have no competing interests.

References

1. Wei Y, Wang L, Jin Z, Jia Q, Brcic L, Akaba T and Chu Q: Biological characteristics and clinical treatment of pulmonary sarcomatoid carcinoma: A narrative review. Transl Lung Cancer Res 13: 635-653, 2024.
2. Smith S, Kao S, Boyer M, Franco M and Moore M: Treatment selection and real-world analysis of immunotherapy with or without chemotherapy in PD-L1-high metastatic non-small cell lung cancer. Intern Med J 54: 1337-1343, 2024.
3. Sun M, She S, Chen H, Cheng J, Ji W, Wang D and Feng C: Prediction model for synergistic anti-tumor multi-compound combinations from traditional Chinese medicine based on extreme gradient boosting, targets and gene expression data. J Bioinform Comput Biol 20: 2250016, 2022.
4. Chang X, Feng X, Du M, Li S, Wang J, Wang Y and Liu P: Pharmacological effects and mechanisms of paeonol on anti-tumor and prevention of side effects of cancer therapy. Front Pharmacol 14: 1194861, 2023.
5. Niu Y, Jin Y, Hao Y, Liang W, Tang F, Qin Z, Liang T and Shi L: Paeonol interferes with lupus nephritis by regulating M1/M2 polarization of macrophages. Mol Immunol 169: 66-77, 2024.
6. Wang Y, Wang Z, Wu X, Zhu S, Guo Q, Jin Z, Chen Z, Zhang D, Hu W, Xu H, *et al*: Paeonol promotes reendothelialization after vascular injury through activation of c-Myc/VEGFR2 signaling pathway. Drug Des Devel Ther 17: 1567-1582, 2023.
7. Zhang JJ, Cai LJ, Pang K, Dong Y, Zhang ZG, Li BB, Li R and Han CH: Paeonol inhibits proliferation and induces cell apoptosis of human T24 and 5637 bladder cancer cells in vitro and in vivo. Clin Transl Oncol 23: 601-611, 2021.
8. Zuo BW, Yao WX, Fang MD, Ren J, Tu LL, Fan RJ and Zhang YM: Boris knockout eliminates AOM/DSS-induced in situ colorectal cancer by suppressing DNA damage repair and inflammation. Cancer Sci 114: 1972-1985, 2023.
9. Du J, Song D, Li J, Li Y, Li B and Li L: Paeonol triggers apoptosis in HeLa cervical cancer cells: The role of mitochondria-related caspase pathway. Psychopharmacology (Berl) 239: 2083-2209, 2022.
10. Zhang L, Chen WX, Li LL, Cao YZ, Geng YD, Feng XJ, Wang AY, Chen ZL, Lu Y and Shen AZ: Paeonol suppresses proliferation and motility of nonsmall-cell lung cancer cells by disrupting STAT3/NF-κB signaling. Front Pharmacol 11: 572616, 2020.
11. Liu LH, Shi RJ and Chen ZC: Paeonol exerts anti-tumor activity against colorectal cancer cells by inducing G0/G1 phase arrest and cell apoptosis via inhibiting the Wnt/β-catenin signaling pathway. Int J Mol Med 46: 675-684, 2020.
12. Cheng CS, Chen JX, Tang J, Geng YW, Zheng L, Lv LL, Chen LY and Chen Z: Paeonol inhibits pancreatic cancer cell migration and invasion through the inhibition of tgf-β1/smad signaling and epithelial-mesenchymal-transition. Cancer Manag Res 12: 641-651, 2020.
13. Cai M, Shao W, Yu H, Hong Y and Shi L: Paeonol inhibits cell proliferation, migration and invasion and induces apoptosis in hepatocellular carcinoma by regulating miR-21-5p/KLF6 axis. Cancer Manag Res 12: 5931-5943, 2020.
14. Chen X, Xu Z, Lu M, Ding W, Zhong J, Deng S, Li S, Miao J, Liu X, Wen Q, *et al*: Paeonol inhibits melanoma growth by targeting PD1 through upregulation of miR-139-5p. Biochem Biophys Res Commu 656: 86-96, 2023.
15. Li M, Cai O, Yu Y and Tan S: Paeonol inhibits the malignancy of Apatinib-resistant gastric cancer cells via LINC00665/miR-665/MAPK1 axis. Phytomedicine 96: 153903, 2022.
16. Wang S, Yang S, Yang X, Deng D, Li J and Dong M: Research progress of traditional Chinese Medicine monomers in reversing multidrug resistance of breast cancer. Am J Chin Med 51: 575-594, 2023.
17. Cai F, Li J, Zhang Y, Huang S, Liu W, Zhuo W and Qiu C: Interaction between Wnt/β-catenin signaling pathway and EMT pathway mediates the mechanism of sunitinib resistance in renal cell carcinoma. BMC Cancer 24: 175, 2024.
18. Cordelli E, Bignami M and Pacchierotti F: Comet assay: A versatile but complex tool in genotoxicity testing. Toxicol Res (Camb) 10: 68-78, 2021.
19. Li R, Chen Y, Yang B, Li Z, Li P, Chen Y, Li J, He J, Wu Y, Sun Y, *et al*: DTX2 promotes glioma development via regulation of HLTF. Biol Direct 19: 2, 2024.
20. Zhang L, Wu L, Zhu X, Mei J and Chen Y: Paeonol represses A549 cell glycolytic reprogramming and proliferation by decreasing m6A modification of Acyl-CoA dehydrogenase. Chin J Physiol 66: 248-256, 2023.
21. Zhang L, Chen WX, Li LL, Cao YZ, Geng YD, Feng XJ, Wang AY, Chen ZL, Lu Y and Shen AZ: Paeonol suppresses proliferation and motility of non-small-cell lung cancer cells by disrupting STAT3/NF-κB signaling. Front Pharmacol 11: 572616, 2020.
22. Zhang C, Zhang J and Guo K: Paeonol upregulates expression of tumor suppressors TNNC1 and SCARA5, exerting anti-tumor activity in non-small cell lung cancer cells. Naunyn Schmiedebergs Arch Pharmacol 397: 5241-5251, 2024.
23. Jensen K, Bikas A, Patel A, Kushchayeva Y, Costello J, McDaniel D, Burman K and Vasko V: Nelfinavir inhibits proliferation and induces DNA damage in thyroid cancer cells. Endocr Relat Cancer 24: 147-156, 2017.
24. Nunna S, Huang YP, Rasa M, Krepelova A, Annunziata F, Adam L, Käppel S, Hsu MH and Neri F: Characterization of novel α-Mangostin and paeonol derivatives with cancer-selective cytotoxicity. Mol Cancer Ther 21: 257-270, 2022.
25. Sheng SQ, Yu LY, Zhou XW, Pan HY, Hu FY and Liu JL: Paeonol prevents migration and invasion, and promotes apoptosis of cervical cancer cells by inhibiting 5-lipoxygenase. Mol Med Rep 23: 401, 2021.
26. Lei Y, Li HX, Jin WS, Peng WR, Zhang CJ, Bu LJ, Du YY, Ma T and Sun GP: The radiosensitizing effect of Paeonol on lung adenocarcinoma by augmentation of radiation-induced apoptosis and inhibition of the PI3K/Akt pathway. Int J Radiat Biol 89: 1079-1086, 2013.
27. Wang Z, Wang X, Rong Z, Dai L, Qin C, Wang S and Geng W: LncRNA LINC01134 contributes to radioresistance in hepatocellular carcinoma by regulating DNA damage response via MAPK signaling pathway. Front Pharmacol 12: 791889, 2022.
28. Chen XM, Jia CL and Zhu ZY: Paeonol impacts ovarian cancer cell proliferation, migration, invasion and apoptosis via modulating the transforming growth factor beta/smad3 signaling pathway. J Physiol Pharmacol 74: 2023.
29. Ekiert H, Klimek-Szczykutowicz M and Szopa A: Paeonia x suffruticosa (Moutan Peony)-A review of the chemical composition, traditional and professional use in medicine, position in cosmetics industries, and biotechnological studies. Plants (Basel) 11: 3379, 2022.
30. Oh JM, Kang Y, Hwang JH, Park JH, Shin WH, Mun SK, Lee JU, Yee ST and Kim H: Synthesis of 4-substituted benzyl-2-triazole-linked-tryptamine-paeonol derivatives and evaluation of their selective inhibitions against butyrylcholinesterase and monoamine oxidase-B. Int J Biol Macromol 217: 910-921, 2022.
31. Wang Y, Li BS, Zhang ZH, Wang Z, Wan YT, Wu FW, Liu JC, Peng JX, Wang HY and Hong L: Paeonol repurposing for cancer therapy: From mechanism to clinical translation. Biomed Pharmacother 165: 115277, 2023.
32. Hao XS, Feng PP, Zhang YY, Wang FZ, Wang GL and Fei HR: Scutebarbatine A induces ROS-mediated DNA damage and apoptosis in breast cancer cells by modulating MAPK and EGFR/Akt signaling pathway. Chem Biol Interact 378: 110487, 2023.

33. Cai J, Chen Y, Wang K, Li Y, Wu J, Yu H, Li Q, Wu Q, Meng W, Wang H, *et al*: Decoding the key compounds and mechanism of Shashen Maidong decoction in the treatment of lung cancer. BMC Complement Med Ther 23: 158, 2023.
34. Kazi M, Alanazi Y, Kumar A, Shahba AA, Rizwan Ahamad S and Alghamdi KM: Oral bioactive self-nanoemulsifying drug delivery systems of remdesivir and baricitinib: A paradigmatic case of drug repositioning for cancer management. Molecules 28: 2237, 2023.
35. Ding M, Shi R, Fu F, Li M, De D, Du Y and Li Z: Paeonol protects against doxorubicin-induced cardiotoxicity by promoting Mfn2-mediated mitochondrial fusion through activating the PKCepsilon-Stat3 pathway. J Adv Res 47: 151-162, 2023.
36. Lv J, Zhu S, Chen H, Xu Y, Su Q, Yu G and Ma W: Paeonol inhibits human lung cancer cell viability and metastasis in vitro via miR-126-5p/ZEB2 axis. Drug Dev Res 83: 432-446, 2022.